Damage quantification in confined ceramics

Cite as: AIP Conference Proceedings **429**, 431 (1998); https://doi.org/10.1063/1.55544
Published Online: 27 March 2008

Yueping Xu, and Horacio D. Espinosa

CP429, *Shock Compression of Condensed Matter – 1997*
edited by Schmidt/Dandekar/Forbes

DAMAGE QUANTIFICATION IN CONFINED CERAMICS

Yueping Xu and Horacio D. Espinosa

School of Aeronautics and Astronautics, Purdue University, West Lafayette, IN 47907

Impact recovery experiments on confined ceramic rods and multi-layer ceramic targets are performed for failure identification and damage quantification. In-material stress measurements with manganin gauges and velocity histories are recorded with interferometric techniques. Observations on recovered samples are made through Optical Microscopy. Microscopy results show that microcracking is the dominant failure mode in ceramic rods and multi-layer ceramic targets. Macrocrack surface per unit area is estimated on various sections along several orientations. Correlation between dynamic loading and crack density is established. Moreover, *multiple penetrator defeat* is observed in ceramic targets recovered from penetration experiments.

INTRODUCTION

In the analysis of damage mechanisms and the formulation of computational models (1), it is of great relevance to determine the number, size and orientation of cracks in the material upon dynamic impact. In this work, damage mechanisms in confined alumina ceramic bars and target plates penetrated by WHA long rods are examined. Stress histories measured with embedded manganin gauges are reported and analyzed. Crack surface area per unit volume on different orientations is characterized quantitatively by stereographic analyses.

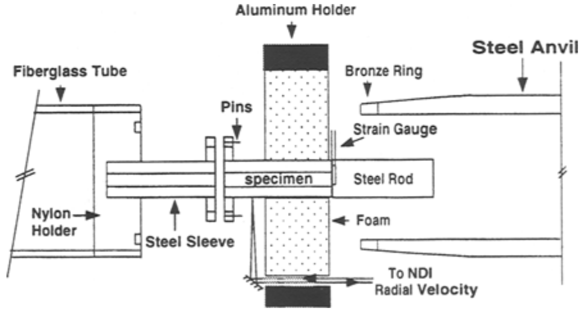

FIGURE 1. Alumina rod on rod recovery experimental configuration.

EXPERIMENTAL METHODS

Case Study I : The test geometry for impact of confined ceramic rods is illustrated in Fig. 1. The alumina rod used in this study, AD-94, was manufactured by Coors Porcelain Company, Golden, CO. The rod was produced with a diameter of 0.5". Lateral confinement, on the surface of the cylindrical ceramic specimen, was obtained by shrink fitting a 4340 steel sleeve with a nominal outer diameter of 1". The sleeve was heated such that the inside diameter expanded to a size slightly larger than the ceramic rod diameter. Then, the ceramic rod was slid into the sleeve. The shrinkage of the sleeve during cooling of the assembly provided the required confinement pressure. Dynamic loading of the ceramic rod was produced by launching a steel rod, mounted on a fiber glass tube, in a light gas gun at Purdue University. The surfaces of the rods were lapped and polished flat. The target was aligned to the impactor surface

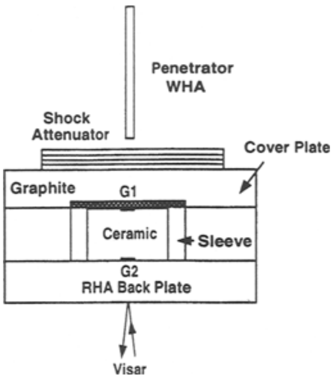

FIGURE 2. Schematic of ballistic experiment.

within 0.5 milliradians by using an optical technique developed by Kumar and Clifton (2). Normal displacement laser interferometry was used to detect the transverse (radial) displacements, at different depths from the impact surface, on the periphery of the sleeve. A distinctive feature of the experiments conducted under this investigation was the recovery of intact specimens. This methodology made it possible to perform extensive microscopic analysis to assess damage. After impact, the sleeve was machined away from the specimen. The rod was sectioned, along the impact axis, grounded, and polished. Chemical etching, by a solution with $HF : HNO_3 : H_2O$ (1:2:5) for 1 minute, was used to reveal the crack pattern.

Case Study II: The test geometry for ballistic impact of confined alumina plates is shown in Fig. 2. Details of the experimental set-up are discussed in (3). After impact, the plates were carefully separated. A two-component epoxy was poured into the cavity, left by the penetrator, to strengthen the fractured ceramic. A diamond saw was used to section the plates on a plane containing the impact direction. To examine the crack pattern, optical microscopy was used. This study provides insight into failure mechanisms and allows the quantification of crack surface area per unit volume.

For estimating the total macrocrack surface area per unit volume, the general relationship, $S_V = 2P_L$ (4), was used. In this formula, S_V is the total crack surface area per unit volume, and P_L is the average value of the number of intersections of a set of test lines of unit length. In principle, the lines can be randomly located with respect to the surfaces of interest. In the case of anisotropic microstructures, the number of intersections of a set of test lines, with the boundaries of macrocracks, depends on the angular orientation of the test lines in the plane. Thus, in order to get a representative average value of the intersection count, it is necessary to perform the measurements on different angular orientations in the different planes. An average of the crack surface per unit volume can be obtained. The dependence of the number of intersections per unit length with the angle of the test array can be used to characterize the degree and type of orientation of a system of lines in a plane. We applied a test array to the system at 30^0, 45^0, 60^0, 90^0, 120^0, 135^0 with respect to the impact direction, and determined P_L separately at each angle θ. From the P_L, we calculated S_V. By plotting S_V versus θ, provides a so-called space rosette which reflected the degree of preferred orientation. For specimens with no preferred orientation, the rosette is a circle. With increasing percentage of preferred crack orientation, the rosette shape is deformed.

EXPERIMENTAL RESULTS AND DISCUSSION

Two rod on rod experiments were performed. The impact velocity for shot 4-1214 was 188 m/sec and for shot 5-0612 was 195 m/sec. For shot 5-0612, the radial velocity was recorded at two points located 12 mm and 15 mm from the impact surface as shown in Fig. 3. The radial velocity at 15 mm has a rising part to a peak velocity of 28 m/sec followed by a decrease and increase resulting from wave release from the sleeve periphery. It should be noted that the radial velocity contains information on the ceramic damage and plastic deformation of the sleeve itself. At approximately 11.5 μsec the trace shows a sudden reduction in particle velocity because of the arrival of an unloading wave from the free end of the impactor rod. Similar features are

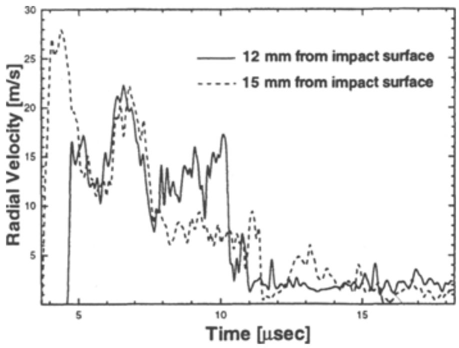

FIGURE 3. Radial velocity history recorded in experiment 5-0612.

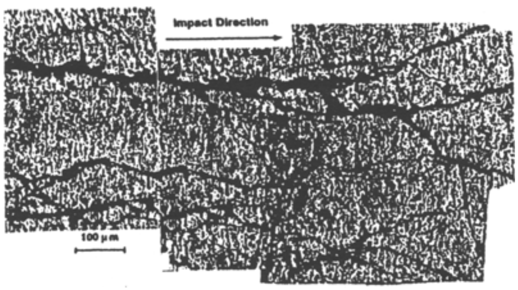

FIGURE 4. Optical micrograph showing macrocrack pattern in recovered rod.

observed in the radial velocity of a point located at 12 mm from the impact surface. A time difference in the arrival of the unloading wave is clearly observed. Further understanding of these traces requires the numerical simulation of the experiments accounting for inelasticity in the ceramic rod and steel sleeve.

Post-test micrographs, of the recovered alumina rod from a region near the impact surface, is shown in Fig. 4. Crack coalescence along the impact direction is observed. The formation of a conical fault, as investigators found in the case of Hopkinson bar experiments (5,6) is not observed. Lack of conical faults can be the result

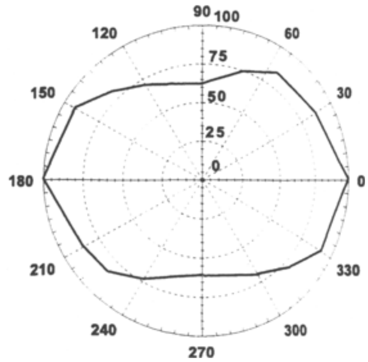

FIGURE 5. Rose of cracks S_V from rod surface sectioned along the impact direction.

of low confining pressure or geometric differences in the specimens. The observed macrocracks in the impact direction are evidence of failure by growth and coalescence of microcracks in planes parallel to the compression axis. Our quantification of crack surface, see Fig. 5, shows that the macrocrack pattern does have a preferred orientation. It is evident that macrocrack density decreases with the increase of the angle, and at 0^0, i.e., along the impact direction, the macrocrack surface area reaches a maximum. However, it should be noted that other orientations, e.g., 45^0 also present a significant S_V.

For the ballistic experiment, observations on polished and etched cross-sections along the penetration direction, revealed a well defined two-layer structure of tungsten alloy entrapped by ceramic fragments at different depth along the penetration direction, see Fig. 6. Since the fragments of the fretted penetrator, from the leading surface, have a high initial forwards velocity, they can travel into open cracks and flow laterally, at the penetrator nose. This observation indicates *multiple penetrator defeat* can be achieved in ceramic targets properly confined. Adjacently to the crater left by the penetrator and along the cover plate-ceramic interface, tungsten particles, with greatly elongated grains, are observed. This is the result of the localized shear deformation experienced by the WHA penetrator. Grain distortion decreases with distance

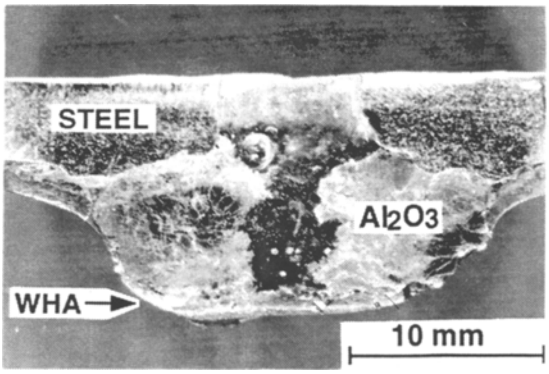

FIGURE 6. Optical micrograph showing penetrator lateral flow at two locations near the ceramic-graphite interface.

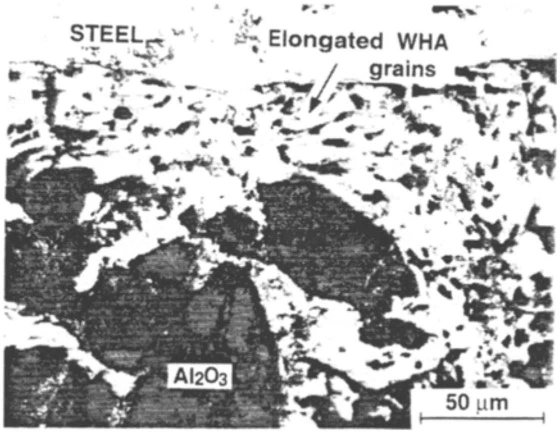

FIGURE 7. Optical micrograph showing penetrator deformation along the steel-ceramic interface.

from the crater as shown in Fig. 7.

Quantification of macrocrack surface area shows that the degree of preferred macrocrack orientation is not as pronounced as in the case of rod on rod impact previously discussed, see Fig. 8. The distribution of macrocracks is close to uniform although the size of fragments is not.

CONCLUSIONS

An attempt to identify failure mechanisms and to quantify crack density in confined alumina rods and plates was made. Fractographic

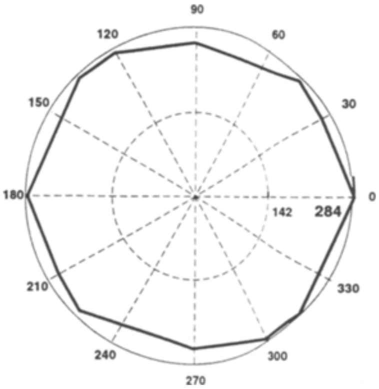

FIGURE 8. Rose of cracks S_V from confined alumina penetration experiment.

observations on penetrated alumina targets show that *multiple penetrator defeat* can be achieved in alumina. The quantification of macrocrack surface area per unit volume, reported in this work, indicates crack patterns with preferred orientations are obtained in confined ceramic rods.

REFERENCES

1. Espinosa, H.D., "On the Dynamic Shear Resistance of Ceramic Composites and its Dependence on Applied Multiaxial Deformation", *Int. J. of Solids and Structures*, Vol. 32, No. 21, 3105, 1995.
2. Kumar, P., Clifton, R.J., 'Optical Alignment of Imapct Faces for Plate Impact Experiments', *J. Appl. Plysics*, **48**, 1366, 1977.
3. Brar, S., Espinosa, H.D., Yuan, G., and Zavattieri, P.D., 'Experimental Study of Interface Defeat in Confined Ceramic Targets', presented at the Shock Compression of Condensed Matter Conference on, Amherst, Massachusetts, 27 July - 1 August 1997.
4. Underwood, E.E., 'Quantitative Stereology' Addison-Wesley, Reading, Mass, pp30-33,1970.
5. Arrowood, R., Lankford, J., 'Compressive Fracture Processes in an Alumina-Glass Composite,' *J. Mater. Sci.*, **22**, 3737, 1987.
6. Chen, W.N., 'Dynamic Failure Behavior of Ceramic Under Multiaxial Compression,' Ph.D. Thesis, Caltech, Pasadena, CA, 1995.